Supplement of Earth Syst. Dynam., 12, 387–400, 2021
https://doi.org/10.5194/esd-12-387-2021-supplement

Supplement of

Seasonal discharge response to temperature-driven changes in evaporation and snow processes in the Rhine Basin

Joost Buitink et al.

Correspondence to: Adriaan J. Teuling (ryan.teuling@wur.nl)

Introduction

This supplement contains additional information to support the descriptions and explanations in the main manuscript. We include the parameter values resulting from the calibration procedure. We show metrics for both the calibration and validation period in all subbasins used in this study. Additionally, we explain how evaporation and snow variables responded to each incremental temperature increase, as we focus only on the most extreme case in the main manuscript.

Text S1, dS2 calibration results

Calibration from the 1250 Latin Hypercube sampling resulted in the following parameters (note that the three g(Q) parameters are defined as a function of slope):

$$\alpha = 0.002472\phi - 3.725, \quad (1)$$

$$\beta = 0.06915\phi + 0.2666, \quad (2)$$

$$\gamma = 0.0316\phi - 0.1622, \quad (3)$$

$$\epsilon = 1.196\ [-], \quad (4)$$

$$\mathrm{dff}_{\mathrm{snow}} = 3.207\ [\mathrm{mm}^{\circ}\mathrm{C}^{-1}\mathrm{day}^{-1}], \quad (5)$$

$$\mathrm{dff}_{\mathrm{glacier}} = 5.523\ [\mathrm{mm}^{\circ}\mathrm{C}^{-1}\mathrm{day}^{-1}], \quad (6)$$

where α, β, and γ are the three g(Q) parameters, ϕ represents the terrain slope in degrees, ϵ represents the the evaporation correction factor, and ddf represents the degree factor for snow and glaciers, respectively. The slope is based on Jarvis et al. (2008), and is calculated at the original resolution of $\pm$80 m. The resulting slope map is resampled to the model resolution.

In Tab. S1, we show the Kling-Gupta efficiencies (KGE) for all basins used in the calibration. The location of these basins within the Rhine is presented in Fig. S1. We also included the KGE for both the 1980s and 2010s period. Due to some limitations in data availability, not all discharge observations covered the entire period. We sliced the timeseries to include most of the available data, yet for some stations it remained impossible to calculate the KGE.

Table S1. Model performance statistics over all subbasins in the Rhine basins. Not all basins had sufficient data to cover the simulation periods, the percentage shows fraction of the period covered by the observations.

Basin	Area (km^2)	KGE calib	KGE 1980s	KGE 2010s
Lobith	168448	0.90 (100%)	0.84 (18%)	0.83 (73%)
Lippe	5520	0.44 (100%)	0.32 (9%)	0.45 (74%)
Ruhr	4320	0.80 (100%)	0.63 (2%)	0.87 (76%)
Sieg	3008	0.73 (100%)	0.80 (9%)	0.86 (74%)
Upper Rhine	145984	0.87 (100%)	-	0.88 (73%)
Lahn	5648	0.59 (99%)	0.49 (9%)	0.73 (72%)
Moselle	28272	0.62 (100%)	0.45 (9%)	0.70 (73%)
Middle Rhine	108672	0.87 (100%)	-	0.81 (73%)
Nahe	4032	0.64 (100%)	-	0.76 (76%)
Maine	28800	0.74 (100%)	0.82 (9%)	0.81 (73%)
Neckar	13456	0.74 (99%)	-	0.78 (73%)
Rhine Valley	53872	0.77 (100%)	-	0.75 (73%)
Switzerland	38832	0.71 (19%)	-	0.68 (69%)

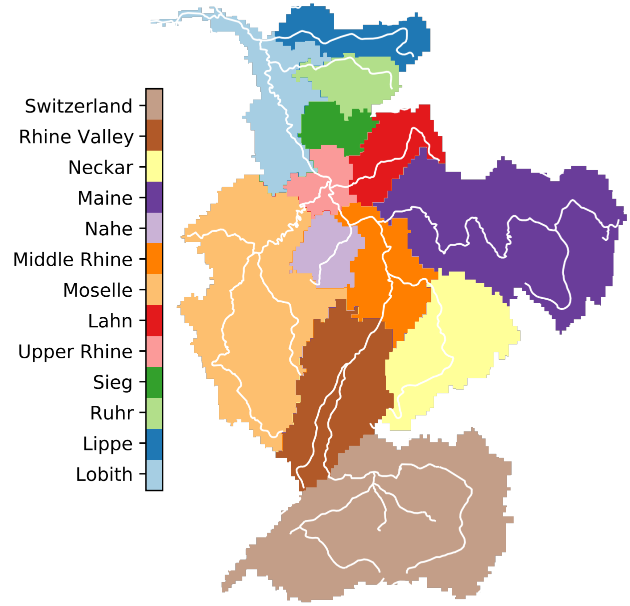

Figure S1. Names and areas corresponding to the (sub-)basins of the Rhine used in this study. The white line indicates the location of the main river network.

Text S2, Temperature induced changes on evaporation and snow

As shown in the manuscript, higher temperatures substantially affect the resulting discharge, where the differences induced by changes in evaporation and snow processes are not constant over the year. To further understand how these processes influence the discharge, the changes in evaporation and snow storage are plotted in Fig. S2 and Fig. S3, respectively.

In Fig. S2, it is visible that potential evaporation will increase with higher temperatures. Despite this, the resulting actual evaporation is not bound to be higher than the 1980s, due to limitations in available soil moisture. This is clearly visible around August 17. Additionally, higher temperatures sometimes hardly change the resulting actual ET, as is the case around August 20. Finally, when sufficient moisture is available for evaporation, higher temperatures will lead to higher actual evaporation rates, as is visible around September 2. The evaporation reduction parameter, indicating the amount of water stress, shows consistently increased reduction with higher temperatures, resulting from the reduced water availability. For most pixels, this relation is non-linear, as it changes from unstressed conditions to water-stressed conditions with higher temperatures.

When investigating the response of snow processes (snowfall and melt from snow and ice) to increased temperatures, results are in line with the expectations, see Fig. S3. Less precipitation is falling as snow (panel a), which means that more precipitation is falling as rain. This has a more direct response to discharge, which explains the increased discharge during winter. Consequently, both the amount of water stored as snow and the fraction the basin covered with snow are reduced (Fig. S3b, c). Snow storages are not only reduced in terms of total water stored, but also depleted more than one month earlier (mid May 1988 versus late June 1988).

With a reduction in snow cover and snow depth in response to higher temperatures, we also see a reduction in basin-averaged snow melt rates (see Fig. S3d). This is the result of a smaller area covered with snow, and hence we see a reduction in basin-averaged snow melt rates. However, the pixels that are covered with snow melt at a faster rate due to the higher temperatures, as can be inferred from the degree-day method to determine snowmelt. This latter effect is visible in the melt from the glaciers (Fig. S3e). With each temperature increase, more meltwater is produced from these glaciers. Eventually, this will lead to a

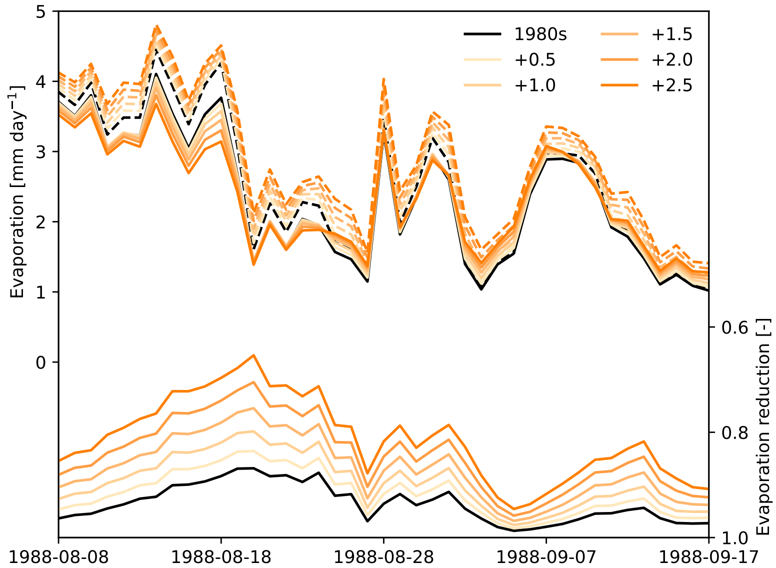

Figure S2. Evaporation differences under increased temperature scenarios. Top half shows potential (dashed) and actual (solid) evaporation, bottom half shows the ratio between actual and potential evaporation. All values are averaged over the entire basin.

reduction in glacier area and volume, and hence a reduction in glacier meltwater production, but this is currently not included in the model.

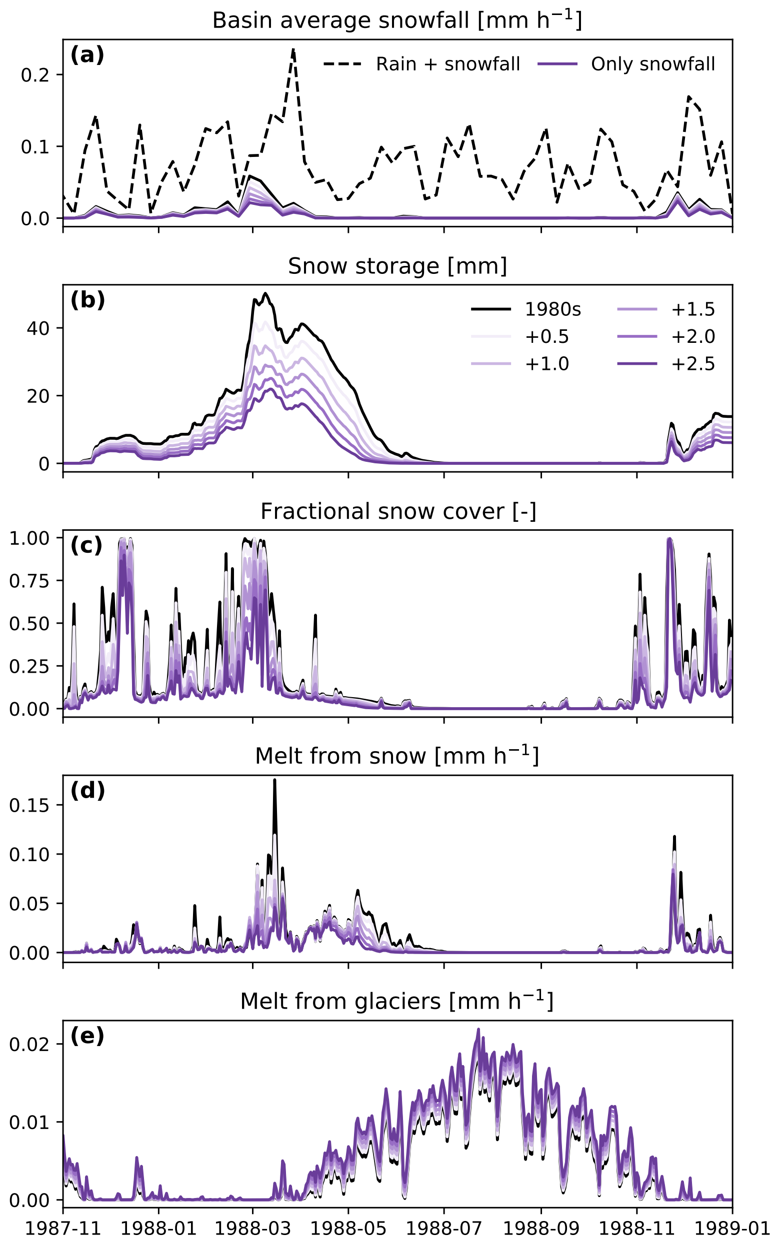

Figure S3. Changes in all considered snow processes under increased temperature scenarios. Panel a shows the amount of snowfall with respect to the total precipitation. Panel b shows the average amount of water stored as snow in snow-covered pixels, and panel c shows the fraction of the basin covered with snow. Panel d and e show the melt rates of snow and ice, respectively, averaged over the entire basin.

References

Jarvis, A., Reuter, H., Nelson, A., and Guevara, E.: Hole-filled SRTM for the globe Version 4, available from the CGIAR-CSI SRTM 90m Database, http://srtm.csi.cgiar.org, 2008.